# Enabling high-sensitivity live single-cell mass spectrometry using an integrated electrical lysis and nano electrospray ionization interface

Pandian, K.; Matos, L.D. de; Hetzel, L A.; Zwier, R.C.T.; Veldhuizen, P.J. van; Schubert, C.; ... ; Hankemeier, T.

Analytica Chimica Acta 1324 (2024) 343068

Contents lists available at ScienceDirect

Analytica Chimica Acta

journal homepage: www.elsevier.com/locate/aca

# Enabling high-sensitivity live single-cell mass spectrometry using an integrated electrical lysis and nano electrospray ionization interface

Kanchana Pandian [a], Luís Daniel de Aguiar Homem e Almeida de Matos [a], Laura A. Hetzel [a], Raphaël Zwier [b], Peter van Veldhuizen [c], Charelle Schubert [a], Jayaprakash Karuppusamy [d], Amy C. Harms [a], Ahmed Ali [a,*], Thomas Hankemeier [a,**]

[a] Metabolomics and Analytics Center, Leiden Academic Centre for Drug Research, Leiden University, Leiden, the Netherlands
[b] Fine Mechanical Department, Leiden Institute of Physics (LION), Leiden University, Leiden, the Netherlands
[c] Electronics Department, Leiden Institute of Physics (LION), Leiden University, Leiden, the Netherlands
[d] Department of Mechanical Engineering, Birla Institute of Technology and Science, Pilani, Hyderabad, India

## HIGHLIGHTS

- The development of the SCEL-nS platform, which integrates single-cell electrical lysis and nano spray techniques.
- Significant reduction in fluorescent intensity post-lysis indicates successful breakdown of the cell membrane.
- Measurement of a single cell spiked with tamoxifen show significant increase in measured peaks compared to non-lysis method.
- Improvement of sensitivity without the need for additional sample dilution.

## GRAPHICAL ABSTRACT

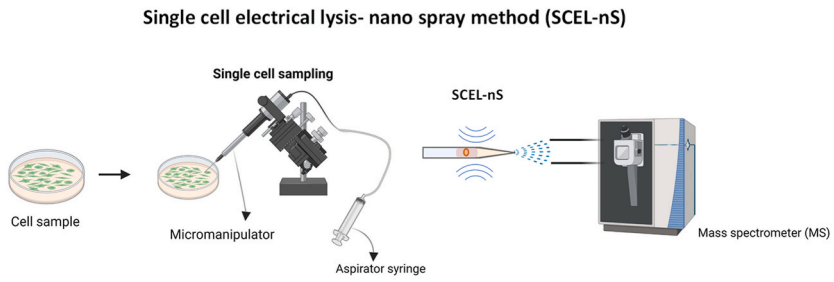


## ARTICLE INFO

Handling Editor: Dr. L. Liang

*Keywords:*
Single-cell metabolomics
Single-cell electrical lysis
Nano spray
Mass spectrometry

## ABSTRACT

*Background:* Live single-cell metabolomic studies encounter inherent difficulties attributed to the limited sample volume, minimal compound quantity, and insufficient sensitivity in the Mass Spectrometry (MS) method used to obtain single-cell data. However, understanding cellular heterogeneity, functional diversity, and metabolic processes within individual cells is essential. Exploring how individual cells respond to stimuli, including drugs, environmental changes, or signaling molecules, offers insights into biology, oncology, and drug discovery. Efficient release of cell contents (lysis) is vital for accurate metabolite detection at the single-cell level. Despite this, traditional approaches in live single cell metabolomics methods do not emphasize efficient lysis to prevent sample dilution. Instead, current live single cell metabolomics methods use direct infusion to introduce the cell into the mass spectrometry without prior chromatographic separation or a lysis step, which adversely affects sensitivity and metabolic coverage.
*Results:* To address this, we developed an integrated single-cell electrical lysis and nano spray (SCEL-nS) platform coupled to an Orbitrap MS capable of efficiently lysing a single cell after being sampled with specially manufactured micropipettes. Lysis efficiency was validated by comparing live cell stain fluorescent intensities of intact

* Corresponding author.
** Corresponding author.
*E-mail address:* ali@lacdr.leidenuniv.nl (A. Ali).

https://doi.org/10.1016/j.aca.2024.343068
Received 3 May 2024; Received in revised form 3 August 2024; Accepted 5 August 2024
Available online 6 August 2024

and electrically lysed cells through microscopy imaging. The SCEL-nS platform successfully induced the breakdown of a single cell, significantly reducing the live cell stain's fluorescent intensity indicating cell membrane breakdown. Additionally, SCEL-nS was validated by measuring single cells spiked with the anti-cancer drug tamoxifen by MS. SCEL-nS use resulted in statistically significant increase in the peak measured by the method compared to the traditional non-lysis method.

*Significance:* Overall, our results demonstrate that the newly incorporated SCEL-nS platform achieved higher sensitivities compared to traditional live single cell analysis methods.

## 1. Introduction

Single-cell metabolomics (SCM) explores metabolites present in individual cells, providing a high-resolution snapshot of the metabolic processes taking place within a cell. Thus, it provides novel insights obtained from individual cells, which offers advantages such as characterization of changes in tumor heterogeneity, quantification of sub populations, and prioritization of the biomarkers of each subpopulation [1–3]. Mass spectrometry (MS) has risen as the method of choice for SCM coupled with a variety of sampling and ionization techniques [4]. Single-cell (SC) MS-based methods can be classified into mass spectrometry imaging techniques, ESI techniques such as laser ablation electrospray ionization mass spectrometry [5], and capillary electrophoresis MS [6]. Despite their utility, these techniques often require extensive sample preparation steps which could cause disruptions to the cell's microenvironment [7].

An alternative technique, termed Live Single-Cell MS (LSC-MS) [8,9] uses a glass capillary to sample a living cell from its microenvironment and directly spray the entire cell into the MS. This method enables the sampling and analysis of individual cells with minimal disruption to the cell or its microenvironment. This technique [10,11], offers a distinct advantage by eliminating the need for elaborate sample preparation steps. Unlike traditional methods, LSC-MS bypasses procedures like matrix removal and derivatization. This allows for the direct infusion of single-cell content into the mass spectrometer, streamlining the analysis and potentially minimizing analyte loss or modification. However, effective cell lysis is crucial in LSC-MS since it ensures a more comprehensive characterization of the intracellular metabolite profile, and it improves the sensitivity, robustness, and quantitative accuracy of measurements. This translates to more reliable and reproducible data acquisition for single-cell metabolomics studies [12–14]. Despite this, a dedicated lysis step has not been included in the traditional LSC-MS workflow to avoid sample dilution. It is therefore necessary to address this technological gap in live single-cell mass spectrometry (MS) methods by incorporating a cell lysis step into LSC-MS.

Conventional cell lysis techniques such as chemical, thermal, acoustic, mechanical, and optical lysis are widely used in SC analysis [15,16]. However, these come with drawbacks making them incompatible with LSC-MS. Ionic detergents are unsuitable for metabolomic analysis [17] due to their interference with MS measurements. While MS-compatible detergents are often utilized for proteomics research [18], using them necessitates dilution of the sample, which limits the detection of low abundance metabolites in single cells. On the other hand, uncontrollable lysis based on osmosis can change the microenvironment and the biochemistry of all cells [19], which adversely affects downstream analysis of said cells. Electrical lysis (EL) is a promising technique that can be seamlessly integrated into live single-cell MS. EL works by subjecting the cell to electric fields, inducing irreversible changes in the permeability of the cell membrane. It does not damage internal cellular components, is highly controlled, does not cause dilution, and is MS compatible [20–22]. However, no current techniques exist that successfully incorporates EL into LSC-MS.

To address this challenge, we have successfully developed and demonstrated the potential of an integrated electrical lysis setup. This single cell electrical lysis and nano spray (SCEL-nS) platform is fully compatible with LSC-MS and similar micro sampling SCM techniques. First, specially designed sampling capillaries were manufactured that can be used for sampling single cells, single cell lysis, and introduction into the MS via nano spray ionization. Then, steady-state numerical simulations were conducted using multi physics software to model the electric potential and field across a cell as it traverses the electrodes. The simulation outcomes were used to design an innovative modified EL and nano spray MS interface. The efficacy of this novel SCEL-nS platform was validated through both fluorescence imaging and MS measurements of single cells spiked with tamoxifen to evaluate the lysis process and the increase in MS signal, respectively.

## 2. Materials and methods

### 2.1. Micropipette fabrication for single cell sampling

#### 2.1.1. Capillary pulling

Special micropipettes needed to be fabricated for single-cell sampling and lysis. For this, the following procedures were performed with GD1.2 capillaries (Narishige, Japan).

The capillaries were shortened to a length of 70 mm with a ceramic cutter stone as shown in the workflow of micropipette fabrication in Fig. 1. A P-97 flaming/brown micropipette puller (P-2000, Sutter Instrument, USA) was used to pull the capillaries into pipettes with long tapers for single cell sampling with the optimized settings shown in Table 1.

#### 2.1.2. Capillary cleaving

A micro forge (MF-900, Narishige, Japan) was used to cleave the capillaries further to obtain the target diameter that is suitable for single-cell sampling (5–7 μm) after pulling (Supplementary Table 1). Micropipettes with a consistent inner diameter (ID) of approximately 2 μm were achieved with good reproducibility, as evidenced by a low standard deviation of ±0.65 (n = 10). Therefore, the capillaries pulled with ~2 μm ID were cleaved using a micro forge to obtain 6.0 ± 1.3 μm ID Supplementary Figs. 1A–D.

#### 2.1.3. Micropipette measurements

The cut capillaries were imaged using a brightfield microscope (EVOS™ Auto 2, Invitrogen, Thermo Fisher Scientific, USA) using 60X magnification with a set scale bar. The capillary images were imported to ImageJ software using the scaling option, and the capillary inner tip diameters were measured by comparing the scale bar length with the length of the inner diameter of the capillary tip (Supplementary Fig. 1D). Only the capillaries with a diameter of 6.0 ± 1.3 μm were used in further experiments.

#### 2.1.4. Capillary coating

To enable capillaries to serve both in the lysis process and as nano spray sources, they must feature a non-conductive section for lysis and a conductive segment for effective nano spray functionality. Before sputtering, the tapered ends of the pipette tips were covered using a metal plate to produce the non-conductive region that can be used in the lysis process (Supplementary Fig. 1E). To achieve the metal coating, the cut glass capillaries were coated with a thin film of conductive material (Platinum/palladium; Pt/Pd sputter target, Ø57 × 0.2 mm Disc - 70-PP5708, EM-Tec, Micro to Nano, Germany).

The deposition of a thin, uniform film was carried out using a spin coater instrument (Model 208HR, No. C5989, Cressington Sputter Coater, UK) under specified parameters: conductivity set to 9.4e+06 S/m, sputter coater thickness set to 40 nm with a tooling factor of 1.6, and a density of 19.52 gm/cm$^3$.

The result of the micropipette fabrication process features a tip diameter measuring 6.0 ± 1.3 μm, with half of it coated with Pt/Pd as shown in Supplementary Fig. 1F.

### 2.2. Electric field simulation and constructing the SCEL-nS platform

Steady-state numerical simulations were performed with COMSOL Multiphysics 5.4 software to simulate the electric potential and electric field in the electrode zone across a cell as it passes the electrodes. To compute the electric potential and electric field, the software is configured with the electrostatic module for simulation. A three-dimensional (3D) geometrical model is generated, and three simulations were carried out: i) a cell positioned near the tip of the micropipette with a cell membrane thickness of 1 μm, ii) a cell membrane thickness of 200 nm, and iii) without a cell. The cell diameter was set to 14 μm and G extra fine meshing was set to the minimum mesh size of 100 nm. The dielectric constant values used in the simulation are as follows, the two L-shaped stainless-steel electrodes = 1.1 x $10^6$, the capillary (borosilicate glass) = 4, the fluid surrounding the cell = 17.5 (HBSS buffer), the cell membrane = 5 [23,24], and cytoplasm = 100 [25,26].

Accurate capillary dimensions were measured using a profile projector (Mitutoyo, The Netherlands) and the dimensions used for simulation. For the electrode and capillary holder design, 3D CAD (Autodesk Inventor Professional) software was used.

### 2.3. Cell culture and sample preparation for electrical lysis validation

Human coronary artery endothelial cells (HCAECs) were used to test the lysis setup. HCAECs (PromoCell, C-12221) were resuspended in 10 ml fresh EGM MV2 medium with supplements (PromoCell, C-22022, C-39216) and cultured in T75 flasks (Nunc Easy flask, Sigma, F7552). Cell cultures were maintained at 37 °C with 5 % $CO_2$ and media was refreshed three times a week. Cells were detached at 85 % confluence with 0.25 % Trypsin EDTA (Lonza, CC-5012) and cell pellets were collected by centrifugation at 300*g* for 5 min. The collected cell pellets were suspended in fresh medium to a concentration of 1 x $10^6$ cells/ml and cultured in 35 mm Petri dishes (60 mm, Sarstedt AG, Germany).

For imaging, cells were stained with the live cell stain – calcein AM (Thermofisher, The Netherlands) of dilution 1:1000 in HBSS and incubated at 37 °C for an hour. If the cells are alive, the nonfluorescent calcein AM is converted to green, fluorescent calcein after acetoxymethyl ester hydrolysis by intracellular esterase. After incubation, the stain solution was removed and washed thrice with HBSS and replaced with 1 mL fresh HBSS for imaging. Before single cell sampling, the cells were imaged to check for the fluorescent intensity using EVOS fluorescent microscope with maximum excitation: 491 nm and maximum emission: 513 nm. For intact cells, either a stained cell or tamoxifen treated cell was first aspirated into a micropipette, followed by the addition of 3 μL of organic solvent. The cell was then imaged using a fluorescence microscope or sprayed to MS. Fig. 5 shows the use of fluorescence for visualizing the intact cell before electrical lysis and the loss of cell integrity after electrical lysis.

**Table 1**
Optimized parameters of micropipette pulling protocol.

| Parameters | Values |
|---|---|
| Heat | Ramp values −12 units |
| pull | 20 units |
| Velocity | 42 units |
| Time | 200 ms |
| Delay | Nil |
| Pressure | 200 pounds |

For MS analysis, cells in 35 mm petri dishes were treated with 3 μM of tamoxifen (T5648, Sigma Aldrich, The Netherlands) for 24 h at 37 °C. After the incubation, cells were washed thrice with HBSS buffer (14025, Thermofisher Scientific, The Netherlands) and cells were ready for single cell sampling.

Single cell sampling was carried out using a micromanipulator attached to a syringe to sample a single cell into the micropipette [8]. The single cell sampling setup is shown in Supplementary Fig. 2.

### 2.4. Electrical lysis and MS method

To lyse the cells, a switch system was integrated to the SCEL-nS platform, which directs the electric current to either lyse a single cell or to spray the cell's content to the MS. After cell lysis 3 μL of organic solvent containing 0.1 % formic acid in 80 % methanol was pipetted into the capillary and the cell was ready either to image using microscope or for the electrospray process.

An orbitrap Exploris 480 (Thermofisher Scientific, USA) was used for MS measurements. Parameters for the acquisition were as follows: mode = positive, spray voltage = 1500 V, Ion Transfer Tube Temp = 400 °C, Resolution = 120,000 FWHM. MS/MS with normalized collision energy of 30 % and an isolation width of 1 Da. The tamoxifen peak was measured based on the 372/72.0807 *m/z* transition.

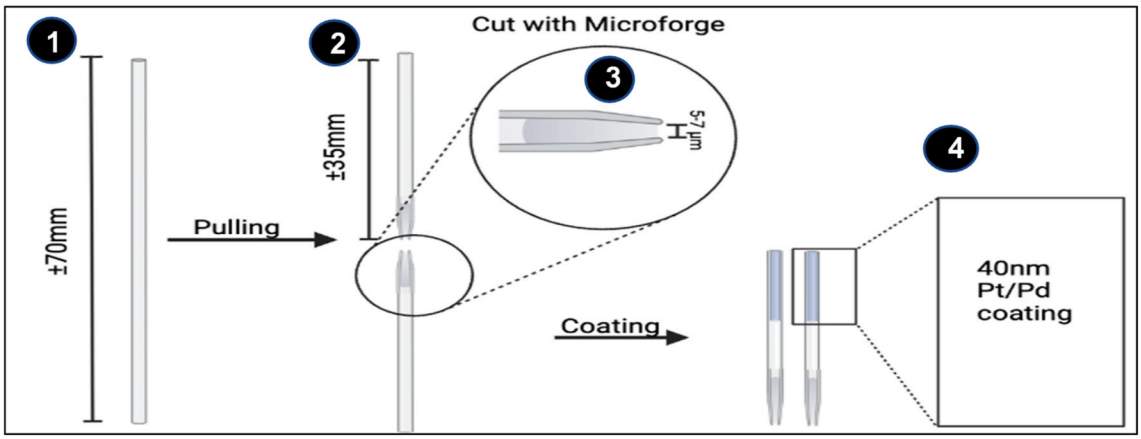


**Fig. 1. Micropipette fabrication workflow and process.** 1) Adjusting optimal length from commercial capillaries. 2) Capillary pulling using Sutter instrument. 3) Capillary cleaving with micro-forge and 4) Micropipette metal (Pt/Pd) coating to obtain electrical conductivity.

### 2.5. Data processing and statistical analysis

After MS measurements, the raw spectra were exported from the manufacturer's raw format to.csv format using Qual browser (Thermofisher Scientific, USA). Each.csv file contained the extracted ion chromatogram (XIC) of the peaks of interest. Average peak intensities were calculated by dividing each peak's total signal by the time a stable spray was observed in each sample. Data analysis and plotting were done using GraphPad Prism (Version 9.3.1).

## 3. Results and discussion

### 3.1. Micropipette fabrication and optimization

Single-cell electrical lysis involves a multi-step process typically encompassing micropipette fabrication, single-cell isolation, pre- and post-lysis imaging using a suitable microscopy technique (SC imaging), and mass spectrometry (MS) analysis. The fabrication process of micropipettes consisted of capillary pulling, cleaving, and metal coating. The dimensions of the micropipette tips were optimized according to the cell size of endothelial cells, which typically have dimensions of approximately 50 μm × 10 μm in culture and 25.8 ± 8.5 μm x 13.2 ± 4.1 μm when in suspension [27]. Our fabrication method was aimed to produce a tip of 5–8 μm ID, which is suitable for both single-cell sampling and nano spray generation. In earlier studies, using similar micropipette fabrication techniques [28,29], single cells were sampled, and the membrane integrity proved to be undamaged [30]. To obtain the optimal tip size of a capillary to sample a single cell, the capillaries were pulled by applying parameters given in the Sutter instrument protocol book such as heat, velocity, pull range, and time/delay. To produce longer tapered and narrowed capillaries, a higher heat setting of 542 units was applied. A pull value of 20 units was established, wherein both filament ends are compressed as the glass softens; the smaller the tip, the higher the pull achieved. Utilizing a higher velocity of 42 units in delayed mode aids in controlling the air-cooling duration and lower pressure units facilitate the creation of long tapered capillaries. Using different combinations of pulling methods and different parameter settings yielded different IDs and SDs of the micropipette presented in the Supplementary Table 1. The optimized parameters can consistently produce micropipettes of mean ID 1.96 μm ± 0.65 (Supplementary Figs. 2A and C). Consistent manufacturing of the micropipettes was achieved with the optimized values shown in Table .1.

To obtain the desired ID 6.0 μm, the pulled capillaries were cleaved at approximately 24 μm of length from the tip of the micropipette with SD of ±2.1 μm. The mean distance and SD required to cleave the capillary from the tip to achieve an inner diameter of 6.0 ± 1.3 μm are presented in Supplementary Table 2. The micro-forge was employed to produce micropipettes with long taper ends and an inner tip diameter of 6.0 μm ± 1.3 (Fig. 2). To confirm the reliability of these procedures and capillary diameter, the cut capillaries were measured using the microscope under brightfield.

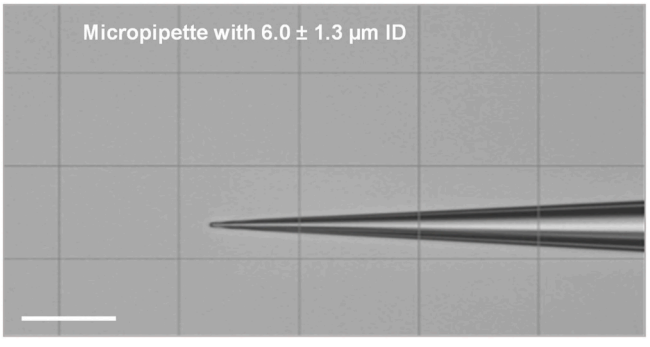


**Fig. 2.** Measurement of capillaries after cleaving step with ideal inner diameter 6.0 ± 1.3 μm using EVOS microscope. Scale bar – 125 μm.

With the optimized protocol, these capillary (6.0 μm ± 1.3) dimensions were suitable for efficient single cell sampling, subsequent lysis, and measurement (Fig. 2).

In addition, the capillary coating with Pt/Pd of 40 nm thickness was effective at transmitting the voltages required for cell lysis and electrospray initiation. In previous studies, Pt/Pd alloy coating on glass substrate has been demonstrated as a suitable choice due to its high electrical conductivity, and resistance to corrosion [31]. Typically, micropipettes for single cell manipulation are crafted with a shorter taper [32,33]. However, in our study, longer taper micropipettes were necessary to achieve the desired size of 6.0 μm with a lower SD (±1.3). This led to the effective sampling of single cells and reduced media pipetting in the capillary due to the small tip diameter while preserving favorable nano spray characteristics.

### 3.2. Electric field simulation for single cell lysis

Prior to the SCEL-nS platform development, numerical simulations were conducted to achieve efficient single-cell lysis by optimizing the design, and comprehending the electric field experienced by the cell. The simulation result aids in estimating the electric field, which helped predict lysis efficiency based on the dielectric properties of the cell and the surrounding environment. The simulation results also helped in determining the transmembrane potential (TMP) across a cell when exposed to an electric field [21,34] and design electrodes to generate efficient electric fields for efficient lysis.

The simulation was performed by giving a positive potential of 500 V to the outer surface of one of the L-shaped electrodes and the other electrode surface is grounded. Three simulations were performed: i) with no cell, and by constructing a pseudo spherical cell with membrane thickness of ii) 1 μm (Fig. 3C) and iii) 200 nm. Electric field simulation and graphical representation of the electric field, and a schematic of the simulation domain were displayed in Supplementary Fig. 3 without the inclusion of a single cell within a micropipette.

The simulation of the electric field and an SC electrical lysis was illustrated in Fig. 3C. The electric field generated by applying 500V across the cell membrane along the axis of the electrode and the capillary exceeds the required range of electric field for SC lysis. The graph of the electric field generated near the wall of the capillary without a single cell showed a maximum of $5 \times 10^5$ V/m. This dropped to $2 \times 10^5$ V/m (Fig. 3C) as a direct consequence of the presence of a cell as it caused a change in the dielectric constant across the capillary. However, the generated EF with the maximum boundary values is sufficient to pass across the TMP of a single cell which agrees with earlier studies showing that $6 \times 10^4$ to $2 \times 10^5$ V/m of electric field strength is required to lyse a single cell [21,34,35]. When the cell membrane thickness was reduced to 200 nm there were no changes in the peak electric field obtained (results are not shown).

With the simulation results, the SCEL-nS platform's electrodes were constructed with the following parameters:

- Electrode length (44.5 mm): Tailored to accommodate the micropipette (Figs. 4A–7) length and maintain proximity to the MS inlet.
- Electrode distance (1.3 mm): Set to achieve adequate electric field strength for the lysis process.
- Adjustment screw (Figs. 4A–8): Utilized to secure the needle, the adjustable screw compensated for slight variations in micropipette length. The design included an adjustment range of approximately 4.5 mm, with a fine thread chosen for the screw to fit snugly into the housing with minimal clearance.

Such parameters were modified based on the simulation result. The newly adapted modified nano spray source is shown in Fig. 4A–E. Within the housing, the electrode tips were fully integrated and equipped with connections for the high-voltage plugs.

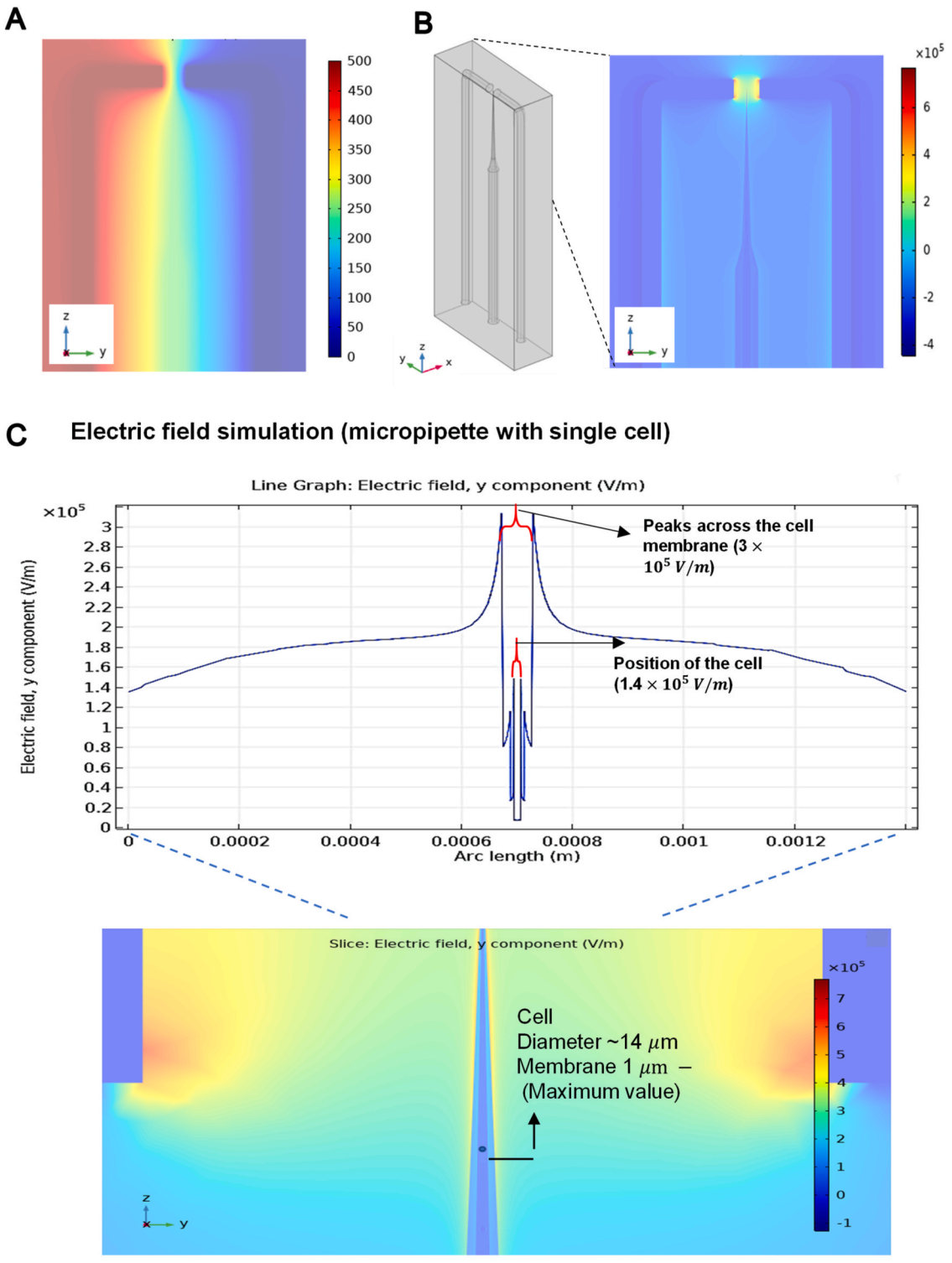


**Fig. 3. Electric field simulation using COMSOL multi physics software.** A) Electric potential across the electrodes with applied voltage (500V). B) The computational field generated with the 3D mesh for the steady-state simulation and electric field (EF) in V/m across the electrodes in the presence of the micropipette. C) Graphical representation of electric field graph and simulation domain schematic, featuring a 14 μm spherical cell positioned within the micropipette. The micropipette is then situated inside the air domain, centrally positioned between a pair of adjacent electrodes. The EF was simulated with the maximum boundary values to obtain optimal field energy to lyse a single cell. EF is represented in V/m.

The simulation results play a crucial role in predicting the lysis efficiency for a single cell electrical lysis/electroporation at an appropriate voltage, thus, achieving efficient lysis instead of allowing the cell membrane to reseal. These predictions are primarily based on the dielectric properties of the cell and the surrounding environment. In general, the simulation results differ depending on whether the cell was in static condition [36] or in movement when it is placed in a suspension liquid [21,37–39]. In our model, when a cell is sampled using a micropipette in a low media volume, it is not possible to restrict the cell's movement. Therefore, maximum boundary values were established to

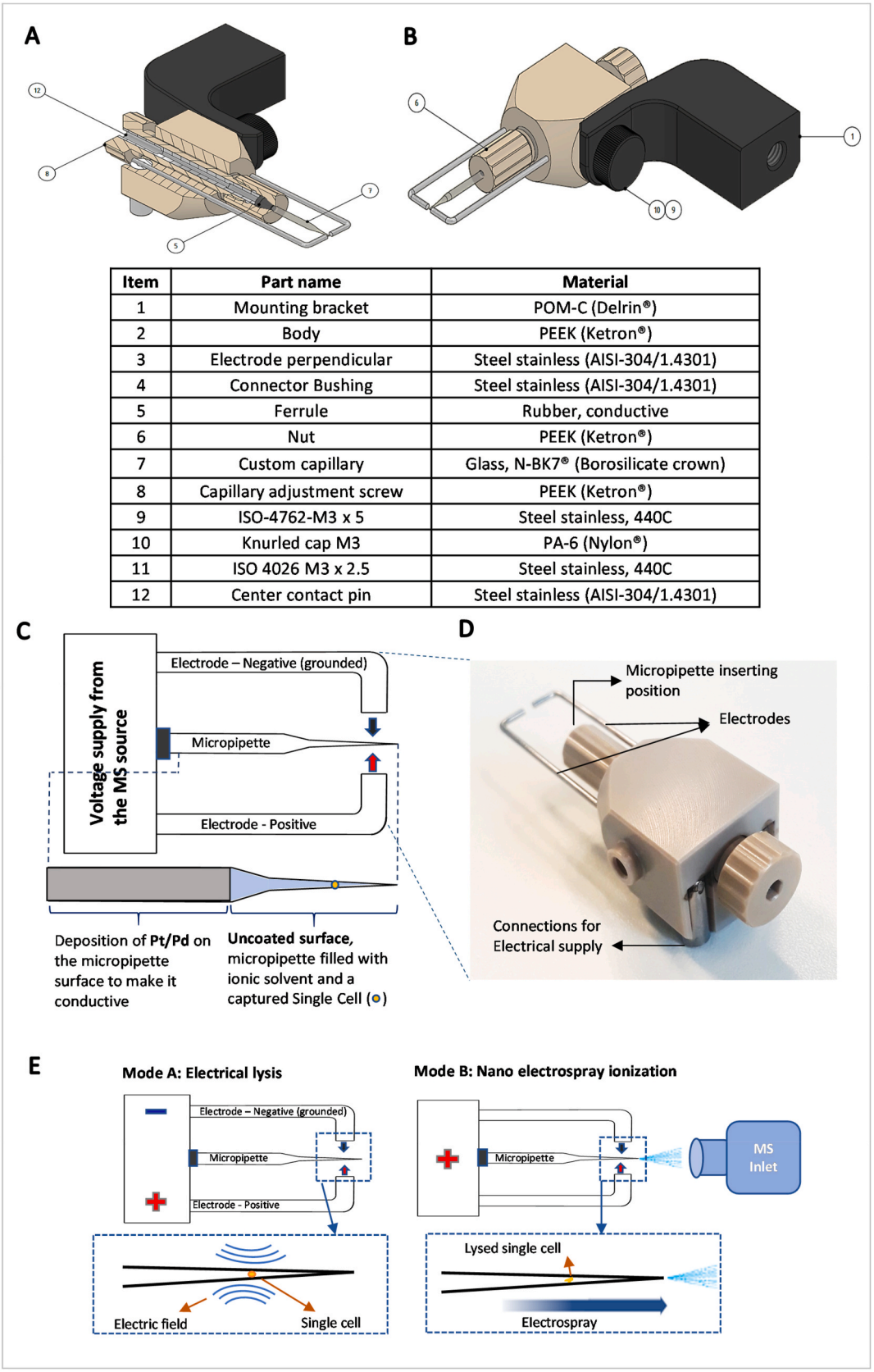


| Item | Part name | Material |
|---|---|---|
| 1 | Mounting bracket | POM-C (Delrin®) |
| 2 | Body | PEEK (Ketron®) |
| 3 | Electrode perpendicular | Steel stainless (AISI-304/1.4301) |
| 4 | Connector Bushing | Steel stainless (AISI-304/1.4301) |
| 5 | Ferrule | Rubber, conductive |
| 6 | Nut | PEEK (Ketron®) |
| 7 | Custom capillary | Glass, N-BK7® (Borosilicate crown) |
| 8 | Capillary adjustment screw | PEEK (Ketron®) |
| 9 | ISO-4762-M3 x 5 | Steel stainless, 440C |
| 10 | Knurled cap M3 | PA-6 (Nylon®) |
| 11 | ISO 4026 M3 x 2.5 | Steel stainless, 440C |
| 12 | Center contact pin | Steel stainless (AISI-304/1.4301) |

**Fig. 4.** A & B) Schematic representation of electrical lysis setup with labelled parts and C) Illustration of the SCEL-nS platform showing the connection to the voltage supply from MS source and the micropipette placement and its conductive region D) Original single-cell electrical lysis and nano spray (SCEL-nS) device and E) Operating the SCEL-nS platform involves employing mode A of the switch system to direct electric current for lysing a single cell. In mode B, the platform electrosprays the content of a single cell into the MS inlet.

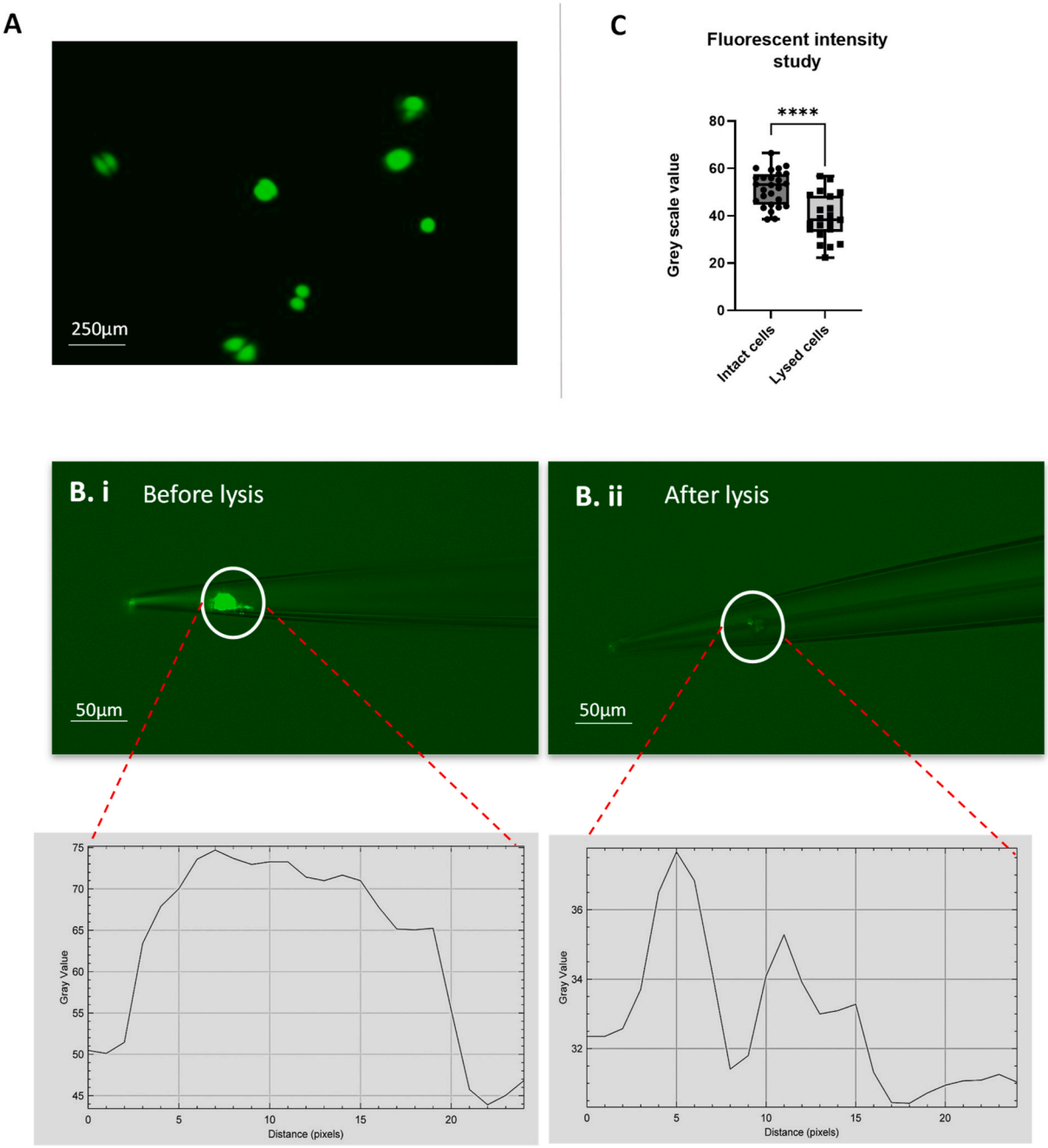


**Fig. 5.** Fluorescent live stain images for lysis validation. *A) Calcein AM stain images of intact cells before sampling, B) Reference image of a single cell within a micropipette i) before and ii) after lysis and the graphical representation of fluorescent intensity is highlighted. Gray values were measured using imageJ software, (gray scale values in pixel units; lysed cell = 38 pixels and for intact cells = 75pixel units) and C) Gray scale intensity calculation of multiple single-cells – intact and lysed cells. A P value was obtained from the student T test. ****, $P < 0.0001$ ($n = 20$).*

get an appropriate electric field (EF) for cell lysis. The electroporation technique employs electrical stimulation to generate enhanced permeability in cell membranes [40]. The conventional EL or electroporation operates with an electric field of a few kilovolts per centimeter in bulk lysis and it perforates the entire population [41], whereas our method works at a single cell level, and the requisite EF can be achieved in less than a kilovolt. Furthermore, our SCEL-nS platform eliminates the need for an additional power supply, as it derives the voltage supply from the MS source, simplifying the design and instrumentation requirements.

### 3.3. Electrical lysis evaluation using microscopic imaging

To evaluate the SCEL-nS platform, microscopic imaging was used to compare individual single cells before and after lysis. Cells were stained with a live cell cytoplasmic dye (Fig. 5A), a single cell was collected in the micropipette, and the fluorescence intensity was assessed before and after lysis using microscopy imaging (Fig. 5B). Results indicated that the cell subjected to EL showed significantly lower fluorescent intensity compared to the intact cell (p value = <0.0001, Fig. 5C).

These results indicated that when the electric field was activated, the cell boundary was weakened due to cell membrane breakdown which led to leakage of the cell cytoplasm to the medium as made evident by

the lower fluorescent intensity (Fig. 5 B&C). Before lysis, the same cells showed adequate membrane integrity as is shown by the higher fluorescent intensity of the cytoplasm-specific stain. This is consistent with previous studies that attempted to use electroporation as a lysis technique [42,43]. In this study, we opted for further confirmation by using mass spectrometry to investigate the effect of the cell lysis on the MS signal.

### 3.4. Evaluation of single-cell electrical lysis using mass spectrometry

To evaluate SC lysis using MS, tamoxifen (3 μM)-treated SCs were sampled in micropipettes using a micromanipulator, EL was performed using SCEL-nS platform and cell contents were infused into the orbitrap. To investigate the lysis efficiency, the tamoxifen signal for each cell was measured using the transition 372/72.0807 *m/z* [11]. Average peak intensities were determined by dividing the total signal of each peak by the elution time.

Results showed higher peak intensity of tamoxifen in lysed cells compared to the non-lysed cells after elution time correction with *P* value = 0.002 obtained from student T-test; Log10FC = 0.2 is shown in Fig. 6.

This outcome suggested that the content of lysed cells dispersed more effectively before detection compared to non-lysed cells that were directly infused.

## 4. Conclusion

Overcoming challenges in metabolomics, sensitivity, and dynamic range is crucial, especially at the single-cell level, where metabolite concentrations can vary from extremely low (nM) to remarkably highly abundant metabolites (mM), metabolite intermediates, signaling compounds, etc. The integrated SCEL-nS platform resulted in higher peak area intensities compared to the traditional LSC-MS methods. In addition, our novel SCEL-nS platform achieves efficient cell lysis with minimal dilution of the cell.

The SCEL-nS platform is not without its limitations, some are shared with other micosampling-based single-cell techniques, while others are unique to SCEL-nS. The current throughput of the method is limited by labor-intensive steps such as manual cell selection and sampling. However, if the sampling, and sample transfer is integrated into a microfluidic system, then in-line lysis can be achieved which will improve sample throughput significantly. Furthermore, implementing an advanced, software-controlled robotic system for cell selection and sampling could significantly address these bottlenecks and improve the platform's overall throughput. Future studies could also expand the platform application to other analytes.

Future applications may extend this approach to various cell types and drug treatments to identify sensitive/low-abundant metabolic biomarkers within heterogeneous subpopulations.

## CRediT authorship contribution statement

**Kanchana Pandian:** Writing – review & editing, Writing – original draft, Visualization, Validation, Methodology, Investigation, Formal analysis, Data curation, Conceptualization. **Luís Daniel de Aguiar Homem e Almeida de Matos:** Methodology, Investigation, Formal analysis. **Laura A. Hetzel:** Methodology, Investigation. **Raphaël Zwier:** Methodology. **Peter van Veldhuizen:** Methodology. **Charelle Schubert:** Methodology. **Jayaprakash Karuppusamy:** Software, Methodology. **Amy C. Harms:** Writing – review & editing, Writing – original draft. **Ahmed Ali:** Writing – review & editing, Supervision, Conceptualization. **Thomas Hankemeier:** Writing – review & editing, Supervision, Funding acquisition.

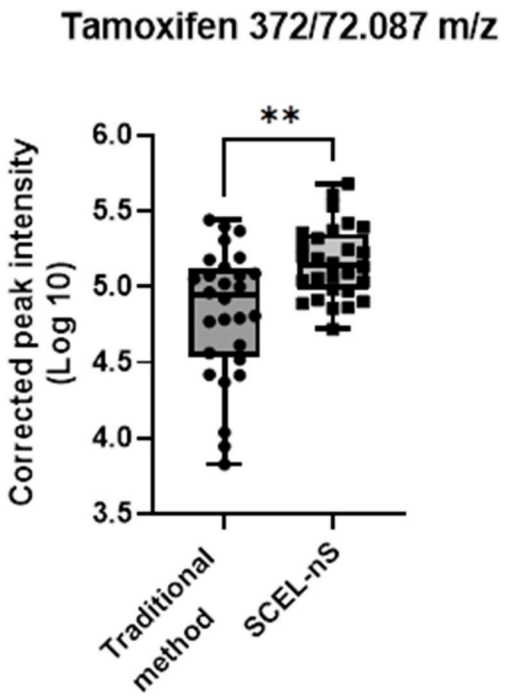


**Fig. 6. Comparison of single cell tamoxifen signal before (using traditional method) and after lysis (using SCEL-nS method).** The peak intensity was corrected with elution time. A p value was obtained from the student T test and Log10FC = 0.2. *, P < 0.05; **, p < 0.001. n = 25–35.

## Declaration of competing interest

The authors declare that they have no conflict of interest.

## Data availability

The data that support the findings of this study are available from Universiteit Leiden on reasonable request.

## Acknowledgements

This project has received funding from the European Union's Horizon 2020 research and innovation program (LogicLab network) under the Marie Skłodowska-Curie grant agreement No 813920 and the NWO XS grant number OCENW.XS23.1.070. We are grateful to Alida Kindt for her insightful review of the manuscript, for Thermo Scientific for the productive discussions and to Judith Verlaan for her contributions to the initial experiments.

## Appendix A. Supplementary data

Supplementary data to this article can be found online at https://doi.org/10.1016/j.aca.2024.343068.

## References

[1] G. Zhu, W. Zhang, Y. Zhao, T. Chen, H. Yuan, Y. Liu, G. Guo, Z. Liu, X. Wang, Single-cell metabolomics-based strategy for studying the mechanisms of drug action, Anal. Chem. 95 (2023) 4712–4720, https://doi.org/10.1021/acs.analchem.2c05351.

[2] R. Liu, J. Li, Y. Lan, T.D. Nguyen, Y.A. Chen, Z. Yang, Quantifying cell heterogeneity and subpopulations using single cell metabolomics, Anal. Chem. 95 (2023) 7127–7133, https://doi.org/10.1021/acs.analchem.2c05245.

[3] D. Wei, M. Xu, Z. Wang, J. Tong, The development of single-cell metabolism and its role in studying cancer emergent properties, Front. Oncol. 11 (2022). https://www.frontiersin.org/articles/10.3389/fonc.2021.814085. (Accessed 6 December 2023).

[4] S. Qin, D. Miao, X. Zhang, Y. Zhang, Y. Bai, Methods developments of mass spectrometry based single cell metabolomics, TrAC, Trends Anal. Chem. 164 (2023) 117086, https://doi.org/10.1016/j.trac.2023.117086.
[5] J.A. Stolee, B. Shrestha, G. Mengistu, A. Vertes, Observation of subcellular metabolite gradients in single cells by laser ablation electrospray ionization mass spectrometry, Angew. Chem. Int. Ed. 51 (2012) 10386–10389, https://doi.org/10.1002/anie.201205436.
[6] H.-W. Liao, S.S. Rubakhin, M.C. Philip, J.V. Sweedler, Enhanced single-cell metabolomics by capillary electrophoresis electrospray ionization-mass spectrometry with field amplified sample injection, Anal. Chim. Acta 1118 (2020) 36–43, https://doi.org/10.1016/j.aca.2020.04.028.
[7] D. Wevers, R. Ramautar, C. Clark, T. Hankemeier, A. Ali, Opportunities and challenges for sample preparation and enrichment in mass spectrometry for single-cell metabolomics, Electrophoresis 44 (2023) 2000–2024, https://doi.org/10.1002/elps.202300105.
[8] T. Fujii, S. Matsuda, M.L. Tejedor, T. Esaki, I. Sakane, H. Mizuno, N. Tsuyama, T. Masujima, Direct metabolomics for plant cells by live single-cell mass spectrometry, Nat. Protoc. 10 (2015) 1445–1456, https://doi.org/10.1038/nprot.2015.084.
[9] T. Masujima, Live single-cell mass spectrometry, Anal. Sci. 25 (2009) 953–960, https://doi.org/10.2116/analsci.25.953.
[10] Y. Abouleila, K. Onidani, A. Ali, H. Shoji, T. Kawai, C.T. Lim, V. Kumar, S. Okaya, K. Kato, E. Hiyama, T. Yanagida, T. Masujima, Y. Shimizu, K. Honda, Live single cell mass spectrometry reveals cancer-specific metabolic profiles of circulating tumor cells, Cancer Sci. 110 (2019) 697–706, https://doi.org/10.1111/cas.13915.
[11] A. Ali, Y. Abouleila, Y. Shimizu, E. Hiyama, T.M. Watanabe, T. Yanagida, A. Germond, Single-cell screening of tamoxifen abundance and effect using mass spectrometry and Raman-spectroscopy, Anal. Chem. 91 (2019) 2710–2718, https://doi.org/10.1021/acs.analchem.8b04393.
[12] A.A. Petelski, N. Slavov, H. Specht, Single-cell proteomics preparation for mass spectrometry analysis using freeze-heat lysis and an isobaric carrier, J. Vis. Exp. 10 (2022) 3791–63802, https://doi.org/10.3791/63802.
[13] Z. Li, Z. Wang, J. Pan, X. Ma, W. Zhang, Z. Ouyang, Single-cell mass spectrometry analysis of metabolites facilitated by cell electro-migration and electroporation, Anal. Chem. 92 (2020) 10138–10144, https://doi.org/10.1021/acs.analchem.0c02147.
[14] Y. Zhu, W. Wang, Z. Yang, Combining mass spectrometry with paternò-büchi reaction to determine double-bond positions in lipids at the single-cell level, Anal. Chem. 92 (2020) 11380–11387, https://doi.org/10.1021/acs.analchem.0c02245.
[15] R.B. Brown, J. Audet, Current techniques for single-cell lysis, J. R. Soc. Interface 5 (2008) S131–S138, https://doi.org/10.1098/rsif.2008.0009.focus.
[16] M. Shehadul Islam, A. Aryasomayajula, P.R. Selvaganapathy, A review on macroscale and microscale cell lysis methods, Micromachines 8 (2017) 83, https://doi.org/10.3390/mi8030083.
[17] D.H. Cheon, S. Lee, W.S. Yang, S. Hwang, H. Jang, M.J. Kim, J.-H. Baek, Optimization of a lysis method to isolate periplasmic proteins from Gram-negative bacteria for clinical mass spectrometry, Proteonomics Clin. Appl. 15 (2021) 2100044, https://doi.org/10.1002/prca.202100044.
[18] Y. Lin, L. Huo, Z. Liu, J. Li, Y. Liu, Q. He, X. Wang, S. Liang, Sodium laurate, a novel protease- and mass spectrometry-compatible detergent for mass spectrometry-based membrane proteomics, PLoS One 8 (2013) e59779, https://doi.org/10.1371/journal.pone.0059779.
[19] Y.-C. Chen, L.-A. Chen, S.-J. Chen, M.-C. Chang, T.-L. Chen, A modified osmotic shock for periplasmic release of a recombinant creatinase from *Escherichia coli*, Biochem. Eng. J. 19 (2004) 211–215, https://doi.org/10.1016/j.bej.2004.03.001.
[20] B. Morshed, M. Shams, T. Mussivand, Electrical lysis: dynamics revisited and advances in On-chip operation, Crit. Rev. Biomed. Eng. 41 (2013) 37–50, https://doi.org/10.1615/critrevbiomedeng.2013006378.
[21] K. Pandian, M. Ajanth Praveen, S.Z. Hoque, A. Sudeepthi, A.K. Sen, Continuous electrical lysis of cancer cells in a microfluidic device with passivated interdigitated electrodes, Biomicrofluidics 14 (2020) 064101, https://doi.org/10.1063/5.0026046.
[22] T. Václavek, F. Foret, Microfluidic device integrating single-cell extraction and electrical lysis for mass spectrometry detection of intracellular compounds, Electrophoresis 44 (2023) 313–322, https://doi.org/10.1002/elps.202100379.
[23] W. Huang, D.G. Levitt, Theoretical calculation of the dielectric constant of a bilayer membrane, Biophys. J. 17 (1977) 111–128.
[24] N. Nasir, M. Al Ahmad, Cells electrical characterization: dielectric properties, mixture, and modeling theories, J. Eng. 2020 (2020) e9475490, https://doi.org/10.1155/2020/9475490.
[25] K.R. Foster, J.M. Bidinger, D.O. Carpenter, The electrical resistivity of cytoplasm, Biophys. J. 16 (1976) 991–1001, https://doi.org/10.1016/S0006-3495(76)85750-5.
[26] W. Liang, X. Yang, J. Wang, Y. Wang, W. Yang, L. Liu, Determination of dielectric properties of cells using ac electrokinetic-based microfluidic platform: a review of recent advances, Micromachines 11 (2020) 513, https://doi.org/10.3390/mi11050513.
[27] B. Garipcan, S. Maenz, T. Pham, U. Settmacher, K.D. Jandt, J. Zanow, J. Bossert, Image analysis of endothelial microstructure and endothelial cell dimensions of human arteries – a preliminary study, Adv. Eng. Mater. 13 (2011) B54–B57, https://doi.org/10.1002/adem.201080076.
[28] M.J. Chen, Y.M. Stokes, P. Buchak, D.G. Crowdy, H.T.C. Foo, A. Dowler, H. Ebendorff-Heidepriem, Drawing tubular fibres: experiments versus mathematical modelling, Opt. Mater. Express, OME 6 (2016) 166–180, https://doi.org/10.1364/OME.6.000166.
[29] M. Han, J. Zhao, J.M. Fabian, S. Mustafa, Y. Ruan, S. Wiederman, H. Ebendorff-Heidepriem, Intracellular delivery of nanoparticles via microelectrophoresis technique: feasibility demonstration, 2020.03.18.996173, https://doi.org/10.1101/2020.03.18.996173, 2020.
[30] M. Nagai, K. Kato, K. Oohara, T. Shibata, Pick-and-Place operation of single cell using optical and electrical measurements for robust manipulation, Micromachines 8 (2017) 350, https://doi.org/10.3390/mi8120350.
[31] R. Heu, S. Shahbazmohamadi, J. Yorston, P. Capeder, Target material selection for sputter coating of SEM samples, Microscopy Today 27 (2019) 32–36, https://doi.org/10.1017/S1551929519000610.
[32] N. Pan, W. Rao, Z. Yang, Single-Probe mass spectrometry analysis of metabolites in single cells, Methods Mol. Biol. 2064 (2020) 61–71, https://doi.org/10.1007/978-1-4939-9831-9_5.
[33] N. Pan, W. Rao, N.R. Kothapalli, R. Liu, A.W.G. Burgett, Z. Yang, The single-probe: a miniaturized multifunctional device for single cell mass spectrometry analysis, Anal. Chem. 86 (2014) 9376–9380, https://doi.org/10.1021/ac5029038.
[34] W. Krassowska, P.D. Filev, Modeling electroporation in a single cell, Biophys. J. 92 (2007) 404–417, https://doi.org/10.1529/biophysj.106.094235.
[35] S. Movahed, D. Li, Microfluidics cell electroporation, Microfluid. Nanofluidics 10 (2011) 703–734, https://doi.org/10.1007/s10404-010-0716-y.
[36] Z. Zhang, T. Zheng, R. Zhu, Single-cell individualized electroporation with real-time impedance monitoring using a microelectrode array chip, Microsyst Nanoeng 6 (2020) 1–10, https://doi.org/10.1038/s41378-020-00196-0.
[37] Y.-J. Lo, U. Lei, A continuous flow-through microfluidic device for electrical lysis of cells, Micromachines 10 (2019) 247, https://doi.org/10.3390/mi10040247.
[38] N. de Lange, T.M. Tran, A.R. Abate, Electrical lysis of cells for detergent-free droplet assays, Biomicrofluidics 10 (2016) 024114, https://doi.org/10.1063/1.4944742.
[39] D.W. Lee, Y.-H. Cho, A continuous electrical cell lysis device using a low dc voltage for a cell transport and rupture, Sensor. Actuator. B Chem. 124 (2007) 84–89, https://doi.org/10.1016/j.snb.2006.11.054.
[40] T. Kotnik, W. Frey, M. Sack, S.H. Meglič, M. Peterka, D. Miklavčič, Electroporation-based applications in biotechnology, Trends Biotechnol. 33 (2015) 480–488, https://doi.org/10.1016/j.tibtech.2015.06.002.
[41] J. Shi, Y. Ma, J. Zhu, Y. Chen, Y. Sun, Y. Yao, Z. Yang, J. Xie, A review on electroporation-based intracellular delivery, Molecules 23 (2018) 3044, https://doi.org/10.3390/molecules23113044.
[42] X. Wei, J. Li, L. Wang, F. Yang, Low-voltage electrical cell lysis using a microfluidic device, Biomed. Microdevices 21 (2019) 22, https://doi.org/10.1007/s10544-019-0369-x.
[43] S. Kemmerling, S.A. Arnold, B.A. Bircher, N. Sauter, C. Escobedo, G. Dernick, A. Hierlemann, H. Stahlberg, T. Braun, Single-cell lysis for visual analysis by electron microscopy, J. Struct. Biol. 183 (2013) 467–473, https://doi.org/10.1016/j.jsb.2013.06.012.